Dalton Transactions

Accepted Manuscript

ROYAL SOCIETY OF CHEMISTRY

www.rsc.org/dalton

Crystal structures and magnetic properties of chiral heterobimetallic chains based on the dicyanoruthenate building block

Jing Ru,[a] Feng Gao,[a] Min-Xia Yao,[b] Tao Wu,[a] and Jing-Lin Zuo*[a]

[a] *State Key Laboratory of Coordination Chemistry, School of Chemistry and Chemical Engineering, Nanjing National Laboratory of Microstructures, Nanjing University, Nanjing 210093, P. R. China*

[b] *School of Science, Nanjing University of Technology, Nanjing 210009, P. R. China*

Abstract

By the reaction of chiral Mn^{III} Schiff-base complexes with the dicyanoruthenate building block, $[Ru(salen)(CN)_2]^-$ ($salen^{2-}$ = N,N'-ethylenebis(salicylideneimine) dianion), two couples of enantiomerically pure chiral cyano-bridged heterobimetallic one-dimensional (1D) chain complexes, $[Mn((R,R)\text{-salcy})Ru(salen)(CN)_2]_n$ (**1**-(*RR*)) and $[Mn((S,S)\text{-salcy})Ru(salen)(CN)_2]_n$ (**1**-(*SS*)) (Salcy = N,N'-(1,2-cyclohexanediylethylene)bis(salicylideneiminato) dianion), $[Mn((R,R)\text{-salphen})Ru(salen)(CN)_2]_n$ (**2**-(*RR*)) and $[Mn((S,S)\text{-salphen})Ru(salen)(CN)_2]_n$ (**2**-(*SS*)) (salphen = N,N'-(1,2-diphenylethylene)bis(salicylideneiminato) dianion), have been synthesized and structurally characterized. Circular dichroism (CD) and vibrational circular dichroism (VCD) spectra confirm the enantiomeric nature of the optically active complexes. Structural analyses reveal the formation of neutral cyano-bridged zigzag single chains in **1**-(*RR*) and **1**-(*SS*), and double chains in **2**-(*RR*) and **2**-(*SS*), respectively. Magnetic studies show that antiferromagnetic coupling are operative between Ru^{III} and Mn^{III} centers bridged by cyanide. Compounds **1**-(*RR*) and **1**-(*SS*) show metamagnetic behavior with a critical field of about 7.2 kOe at 1.9 K resulted from the intermolecular $\pi\cdots\pi$ interactions. Additionally, magnetostructural correlation for some typical cyano-bridged heterobimetallic Ru^{III}–Mn^{III} compounds is discussed.

* To whom correspondence should be addressed. Email: zuojl@nju.edu.cn; Fax: +86-25-83314502. Nanjing University.

Introduction

Low-dimensional magnetic materials, such as single-molecule magnets (SMMs) and single-chain magnets (SCMs) with slow magnetic relaxation behavior, have been extensively studied due to their unique potential applications for molecular devices, high-density information storage, and quantum computers.[1] SMMs and SCMs are constructed based on various organic ligands and paramagnetic metal ions. As a representative, cyanometallates have been widely used to prepare molecule-based magnetic materials in which cyanide unit can mediate efficient ferro- or antiferromagnetic exchange interactions between paramagnetic metal centers.[2,3] In addition to well-known cyanometallates including 3d transition metals, 4d or 5d cyanometallates have been also reported with various SMM, SCM, spin-canting, or metamagnetic characters.[4,5] The use of heavier transition metal ions offers an extra benefit: presence of more diffuse 4d (or 5d) orbitals providing stronger exchange interactions.[6,7]

For new molecule-based materials with more diversified properties, one of the goals is to prepare materials that possess not only one expected property of function but also combine two or more of them in a multifunctional system. In particular, due to possible application in a variety of new technologies, the synthesis of materials with both chirality and magnetism has attracted more attention in last decades.[8-10] Several cyanide-bridged chiral magnetic complexes have been successfully synthesized with poly-cyanometalates as bridging units and unsaturated transition-metal complexes containing chiral coligands as assembled segments.[11-13] More recently, a pair of one-dimensional enantiomers based on the versatile chiral dicyanoruthenate(III) building block have been synthesized by us, and they are chiral single-chain magnets with the effective spin reversal barrier of 28.2 K.[14] For more studies on homochiral heterobimetallic compounds and further elucidating the magneto-structural correlation in 4d cyanometallates systems, in this paper, the anionic *trans*-dicyanometalate building block $[Ru(salen)(CN)_2]^-$ and cationic manganese(III) chiral Schiff-base compound (Scheme 1) were assembled, resulting

into the formation of two couples of enantiomerically pure chiral cyano-bridged heterobimetallic one-dimensional chain complexes $[Mn((R,R)\text{-salcy})Ru(salen)(CN)_2]_n$ (**1**-(*RR*)) and $[Mn((S,S)\text{-salcy})Ru(salen)(CN)_2]_n$ (**1**-(*SS*)), $[Mn((R,R)\text{-salphen})Ru(salen)(CN)_2]_n$ (**2**-(*RR*)) and $[Mn((S,S)\text{-salphen})Ru(salen)(CN)_2]_n$ (**2**-(*SS*)), respectively. Their crystal structures, CD spectra, VCD spectra, selected IR data and magnetic properties are described. To our knowledge, the reports on chiral magnetic complexes assembled from the cyanoruthenate(III) building block are still limited.[14] The metamagnetic behavior for compounds **1**-(*RR*) and **1**-(*SS*) at low temperature is due to the relatively strong interchain π···π interactions.

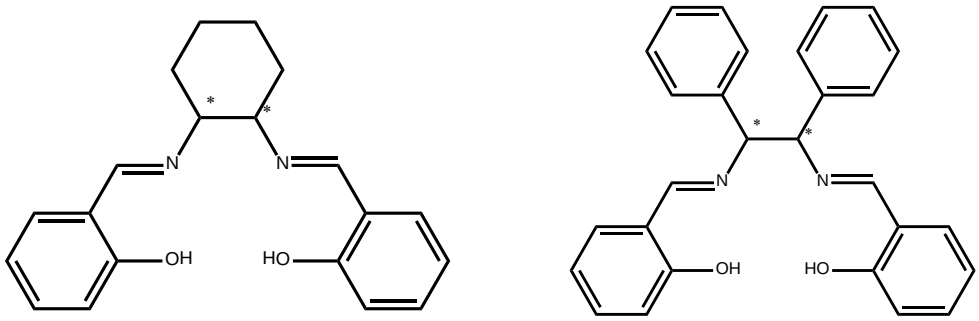

$_{(R,R)}$-or $_{(S,S)}$-H_2Salc_y $_{(R,R)}$-or $_{(S,S)}$-H_2Sal_phen

Scheme 1

Experimental Section

Starting materials

All reagents and solvents were commercially available and used as received without further purification. (*R*,*R*)- and (*S*,*S*)- $[Mn(salcy)(H_2O)_2]ClO_4$, (*R*,*R*)- and (*S*,*S*)- $[Mn(salphen)(H_2O)_2]ClO_4$ and $[(n\text{-}Bu)_4N][Ru(salen)(CN)_2]$ were prepared according to the published methods.[15,16] (*R*,*R*)- and (*S*,*S*)-H_2salcy and (*R*,*R*)- and (*S*,*S*)-H_2salphen (Scheme 1), were synthesized from the condensation of salicylaldehyde with 1,2-diaminocyclohexane or 1,2-diphenylethylenediamine in a molar ratio of 2:1 in ethanol, respectively.

Caution! Although no problems were encountered in this work, perchlorate salts are potentially explosive and cyanides are very toxic. Thus, these starting materials should be handled in small quantities and with great care.

Preparation of [Mn((*R,R*)-salcy)Ru(salen)(CN)$_2$]$_n$ (1-(*RR*)). A solution of [Mn((*R,R*)-salcy)(H$_2$O)$_2$]ClO$_4$ (20.4 mg, 0.04 mmol) in 10 mL of methanol was added to a solution of [(*n*-Bu)$_4$N][Ru(salen)(CN)$_2$] (26.50 mg, 0.04 mmol) in 10 mL of acetonitrile. After 30 min of stirring, the resulting green solution was filtered and then left undisturbed. The slow evaporation of the filtrate at room temperature gave dark-green needles crystals of **1**-(*RR*) after two weeks. Yield: 60%. Anal. Calcd for $C_{38}H_{34}MnN_6O_4Ru$: C, 57.43; H, 4.31; N, 10.57. Found: C, 57.12; H, 4.01; N, 10.72. Selected IR data (KBr, cm^{-1}): 2161 (ν(C≡N)).

Preparation of [Mn((*S,S*)-salcy)Ru(salen)(CN)$_2$]$_n$ (1-(*SS*)). Preparation was similar to that of **1**-(*RR*) with the exception [Mn((*S,S*)-salcy)(H$_2$O)$_2$]ClO$_4$ was used. After 30 min of stirring, the resulting green solution was filtered and then left undisturbed. The slow evaporation of the filtrate at room temperature gave dark-green needles crystals of **1**-(*SS*) after two weeks. Yield: 60%. Anal. Calcd for $C_{38}H_{34}MnN_6O_4Ru$: C, 57.43; H, 4.31; N, 10.57. Found: C, 57.13; H, 4.03; N, 10.78. Selected IR data (KBr, cm^{-1}): 2161 (ν(C≡N)).

Preparation of [Mn((*R,R*)-salphen)Ru(salen)(CN)$_2$]$_n$ (2-(*RR*)). A solution of [Mn((*R,R*)-salphen)(H$_2$O)$_2$]ClO$_4$ (24.8 mg, 0.04 mmol) in 10 mL of methanol was added to a solution of [(*n*-Bu)$_4$N][Ru(salen)(CN)$_2$] (26.50 mg, 0.04 mmol) in 10 mL of methanol. After 30 min of stirring, the resulting green solution was filtered and then left undisturbed. The slow evaporation of the filtrate at room temperature gave dark-green needles crystals of **2**-(*RR*) after two weeks. Yield: 55%. Anal. Calcd for $C_{92}H_{72}Mn_2N_{12}O_8Ru_2$: C, 61.88; H, 4.06; N, 9.41. Found: C, 61.72; H, 4.32; N, 9.23. Selected IR data (KBr, cm^{-1}): 2101 (ν(C≡N)).

Preparation of [Mn((*S,S*)-salphen)Ru(salen)(CN)$_2$]$_n$ (2-(*SS*)). Preparation was similar to that of **2**-(*RR*) with the exception [Mn((*S,S*)-salphen)(H$_2$O)$_2$]ClO$_4$ was used. After 30 min of stirring, the resulting green solution was filtered and then left undisturbed. The slow evaporation of the filtrate at room temperature gave dark-green

needles crystals of **2**-(*SS*) after two weeks. Yield: 55%. Anal. Calcd for $C_{92}H_{72}Mn_2N_{12}O_8Ru_2$: C, 61.88; H, 4.06; N, 9.41. Found: C, 61.73; H, 4.31; N, 9.22. Selected IR data (KBr, cm^{-1}): 2101 (ν(C≡N)).

X-ray Structure Determination. The crystal structures were determined with a Siemens (Bruker) SMART CCD diffractometer using monochromated Mo Kα radiation (λ = 0.71073 Å). The cell parameters were retrieved using SMART software and refined using SAINT[17] for all observed reflections. Data was collected using a narrow-frame method with scan widths of 0.30° in ω and an exposure time of 10 s/frame. The absorption corrections were applied using SADABS[18] supplied by Bruker. Structures were solved by direct methods using the program SHELXL-97.[19] The positions of metal atoms and their first coordination spheres were located from direct methods E-maps. The other non-hydrogen atoms were found in alternating difference Fourier syntheses and least-squares refinement cycles and, during the final cycles, refined anisotropically. Hydrogen atoms were placed in calculated positions and refined as riding atoms with a uniform value of U_{iso}. Final crystallographic data and values of R_1 and wR_2 are listed in Table 1. Selected bond distances and angles for complexes **1**-(*RR*) - **2**-(*SS*) are listed in Tables 2-3 and S1-S2,† respectively. CCDC reference numbers are 1019502 (**1**-(*RR*)), 1019503 (**1**-(*SS*)), 1019504 (**2**-(*RR*)), and 1019505 (**2**-(*SS*)).

Physical Measurements. Elemental analyses for C, H and N were performed on a Perkin-Elmer 240C analyzer. CD spectra were recorded on a Jasco J-810 spectropolarimeter. IR and VCD spectra in the region of 1800–800 cm^{-1} were recorded on a VERTEX 80v Fourier transform infrared spectrometer equipped with a PMA 50 VCD/IRRAS module (Bruker, Germany) using previous procedures.[20] The solid samples were prepared by mixing the compound and KBr in a 1:200 ratio, and pressing the pellet in a Perkin Elmer hydraulic pellet press for 5 min under 10 tons of pressure. The photo elastic modulator (PEM) was set to 1500 cm^{-1}, and the spectral resolution was 4 cm^{-1}. All VCD measurements were collected for 1 h composed of 4 blocks in 15 min. Baseline correction was performed with the spectra of pure KBr pellet using the same measurement setup. Magnetic susceptibilities for polycrystalline

samples were measured with the use of a Quantum Design MPMS-SQUID-VSM magnetometer in the temperature range 1.9–300 K. Field dependences of magnetization were measured using Quantum Design MPMS-SQUID-VSM system in an applied field up to 70 kOe.

Results and discussion

Spectroscopic and Ferroelectric Studies

The Circular dichroism (CD) spectra measurements in KBr pellets confirm the optically activity and enantiomeric nature of **1**-(*RR*) and **1**-(*SS*), **2**-(*RR*) and **2**-(*SS*) (Figures S1-S2, ESI†). The CD spectrum of **1**-(*RR*) (*R* isomer) exhibits a negative Cotton effect at λ_{max} = 331, 406, 595 nm, and a positive dichroic signal centered at 273 nm, while **1**-(*SS*) (*S* isomer) shows Cotton effects of the opposite sign at the same wavelengths. **2**-(*RR*) (*R* isomer) exhibits a negative Cotton effect at λ_{max} =318 nm, 510 nm, and a positive dichroic signal centered at 269 nm, while **2**-(*SS*) (*S* isomer) shows Cotton effects of the opposite sign at the same wavelengths. Comparing the CD spectra of the ligands and the corresponding metal complexes, it is confirmed that the chirality is transferred from the ligand to the complexes: the strong absorption bands at high energy (λ < 450 nm) that can be assigned to the intra-ligand transitions, and the new broad band in the visible region is attributable to an admixture of metal-to-ligand charge-transfer.[21] Similar red shifts are also observed in other Mn(III) salen complexes.[11a-11d]

Vibrational circular dichroism (VCD) is the extension of CD into infrared region of the spectrum reflecting vibrational transitions, has been testified as a powerful technique in the structural analysis of chiral molecules.[22] As expected, the IR spectra of both enantiomers are almost the same, while the VCD spectra are nearly mirror images (Fig. 1). In the IR spectra, the feature absorptions come from the imine double bonds stretch vibrations (1632, 1606 cm^{-1} for **1**-(*RR*) and **1**-(*SS*)**,** 1613, 1597 cm^{-1} for **2**-(*RR*) and **2**-(*SS*), and C−H deformations (1542, 1524, 1310 and 1291 cm^{-1} for **1**-(*RR*) and **1**-(*SS*), 1537, 1438, 1294 cm^{-1} for **2**-(*RR*) and **2**-(*SS*)). In the corresponding VCD spectra, the two imine chromophores manifest as a couplet curve, while the latter

display as incisive peaks.

Given above complexes crystallize in a chiral space group, their second-order nonlinear optical (NLO) properties were studied. The results from the powdered sample indicate that **1**-(*RR*)-**2**-(*SS*) show NLO effect with approximate responses of 0.3 times that of urea. Although **2**-(*RR*) and **2**-(*SS*) crystallize in a polar point group (*C*1) required for ferroelectric behavior, however, no large single crystal suitable for detailed ferroelectric measurements are obtained.

Structural Description

1-(*RR*) and **1**-(*SS*) are a pair of enantiomers and crystallize in the chiral space group $P2_1$ (Fig. 2). They are made up of a neutral cyano-bridged zigzag chain with $(-Ru-C\equiv N-Mn-N\equiv C-)_n$ as repeating unit, in which two neighboring Mn(III) ions in a *trans* mode. Here, only the crystal structure of **1**-(*RR*) is described in detail (Figure 4). The Ru(III) ion possesses a slightly distorted octahedral coordination environment, bonded by two N atoms (salen ligand), two C (cyanide groups) and two O atoms (phenolic oxygen). The average Ru−N(O) bond length 2.01(4) Å, whereas the mean Ru-C distance is 2.079(4) Å. This trend agrees well with other Ru^{III}-M bimetallic compounds.[4e] The Ru−C≡N angles (174.2(4)–175.4(6)°) show slight deviation from linearity. In the $[Mn(salcy)]^+$ unit, the Mn(III) ion situates in an obviously distorted octahedral geometry based on equatorial N_2O_2 donor atoms from salcy (Mn1−O3 = 1.863(4) Å, Mn1−O4 = 1.880(4) Å, Mn1−N3 = 2.002(4) Å, and Mn1−N4 = 1.963(5) Å) and two apical N atoms from bridging CN groups (Mn1−N5 = 2.325(4) Å and Mn1−N6 = 2.354(4) Å). The axial elongation results from the well-known Jahn-Teller effect on an octahedral high-spin Mn(III) ion.[4c,4e,14] The Mn–N≡C bond angles deviate significantly from linearity with the angles of 156.4(4)° for C38-N5-Mn1 and 154.3(4)° for C37#2-N6-Mn1 (symmetric operation #2: x+1, y, z). The chains are running along the *c* axis with the intrachain Ru–Mn separation of 5.400(3) Å through bridging cyanide. The shortest interchain Ru···Ru, Mn···Mn, and Ru···Mn distances are 7.422, 7.445, 7.005 Å, respectively, obviously longer than the intrachain metal-metal distance. Each chain interacts with two other adjacent chains by π···π stacking between aromatic rings of the salcy ligand with a centroid distance of 3.89 Å, thus forming the 2D structure (Supporting Information, Figure S5).

Complexes **2**-(*RR*) and **2**-(*SS*) are also enantiomers but crystallize in chiral space group *P*1 (Fig. 3). They are made up of neutral cyano-bridged zigzag double chains with $(-Ru-C\equiv N-Mn-N\equiv C)_n$. As shown in Figure 5, in complex **2**-(*RR*), the crystallographically independent unit contains two types of $[Ru(salen)CN_2]^-$ anions (including Ru1 and Ru3 atoms, respectively). Both Ru1 and Ru2 ions possess a slightly distorted octahedral coordination environment, and the Ru−C (cyano) (2.017(7) − 2.136(6) Å) and Ru−N (salen) (2.017(5) − 2.016(6) Å) and Ru−O (salen) (2.016(6) − 2.245(6) Å) bond lengths are within the normal values. The Ru−C≡N angle (167.4(6) – 178.0(5)°) shows slight deviation from linearity. There are also two crystallographically independent Mn(III) ions in **2**-(*RR*), Mn1 and Mn3. Both Mn(III) ions have an obviously distorted octahedral geometry with the equatorial plane occupied by N_2O_2 atoms from the salphen ligand and the two cyanide nitrogen atoms. Because of the Jahn-Teller distortion of the Mn(III) ions, the axial bond lengths (2.272(6) Å and 2.299(6) Å for Mn1, 2.331(6) Å and 2.349(7) Å for Mn3) are relatively longer than the equatorial ones (2.019(5) – 2.065(6) Å for Mn1 and 2.010(6) – 2.016(5) Å for Mn3), but comparable to the reported Ru^{III}-Mn^{III} complexes $\{Ru^{III}(Q)_2](\mu\text{-}CN)_2[Mn^{III}(L^1)]\}_n$ (Q = the anion of 8-hydroxyquinoline, L^1 = N,N'-(1,2-cyclohexanediyl-ethylene)bis(salicylideneiminato)dianion).[4e] The Mn–N≡C angles deviate significantly from linearity with the Mn1−N≡C angles (166.0(4) and 171.0(5)°) and the Mn3–N≡C angles (158.7(6) and 174.8(5)°), which are larger than those of $\{Ru^{III}(Q_2)](\mu\text{-}CN)_2[Mn^{III}(L^1)]\}_n$ (154.18° and 149.62°).[4e] The Ru1-Mn1 and Ru3-Mn3 atoms are linked by cyanide to form 1D infinite chain along the *b* axis. There are no obvious interactions between two neighboring chains. The shortest interchain Ru···Ru, Mn···Mn, and Ru···Mn distances are 7.173, 7.135, 6.268 Å.

Magnetic Properties

Magnetic susceptibility measurements were performed on polycrystalline samples of complexes **1**-(*RR*) and **2**-(*RR*) using the SQUID magnetometer at temperatures ranging from 1.9 to 300 K.

The temperature-dependent $\chi_M T$ values of **1**-(*RR*) are displayed in Fig. 6. At 300 K, the $\chi_M T$ value of 3.30 $cm^3 \cdot K \cdot mol^{-1}$ for per $Ru^{III}Mn^{III}$ unit is close to 3.38 $cm^3 \cdot K \cdot mol^{-1}$ expected for one low-spin Ru(III) center (S = 1/2) and one high-spin Mn(III) center (S = 2) assuming g = 2.00 and no exchange coupling. Upon cooling,

the $\chi_M T$ values decreases smoothly and attains a minimum value of 2.06 $cm^3 \cdot K \cdot mol^{-1}$ at 3.4 K, indicating the presence of antiferromagnetic coupling between the cyanide-bridged Ru(III)-Mn(III). Upon further cooling, it increases sharply to reach a maximum value of 2.30 $cm^3 \cdot K \cdot mol^{-1}$ at 3.0 K. Then it decreases at lower temperature to reach 1.54 $cm^3 \cdot K \cdot mol^{-1}$ at 1.9 K. The magnetic susceptibility above 30 K conforms well to the Curie-Weiss law and gives the Curie constant of 3.33 $cm^3 \cdot K \cdot mol^{-1}$ and a Weiss constant of −2.38 K (Figure S5, ESI†). The negative θ indicates dominant antiferromagnetic (AF) coupling between spin centers.

According to the structure, an approximate Hamiltonian can be described as $H = -J\sum_i S_{Rui} \cdot [(1+\alpha)S_{Mni} + (1-\alpha)S_{Mni+1}]$ [23], where the local spins are S_{Ru} and S_{Mn}, the local Zeeman factors g_{Ru} and g_{Mn}, and the couplings between nearest neighbors $J(1+\alpha)$ and $J(1-\alpha)$. The best fit between 30 and 300 K gives g_{Mn} = 1.99, g_{Ru} = 1.98, J = −0.86 cm^{-1}, α = 0.53 and zJ' = 0.3 ($R = 1.17 \times 10^{-4}$). The result confirms that antiferromagnetic couplings between Ru^{III} and Mn^{III} ions within the chain are operating.

The field dependent magnetization for **1**-(*RR*) was measured up to 70 kOe at 1.9 K (Fig.7). The curve at 1.9 K presents a sigmoid shape, typical of metamagnetic behavior: the magnetization first increases slowly with increasing magnetic field until 5 kOe due to the relatively strong intermolecular π···π interactions, then increases abruptly for a phase transition, and finally attains to a maximum value of 2.92 Nβ at 70 kOe.[4e] From the variable-temperature magnetization measurements at different low fields and dM/dH vs H plot at 1.9 K (inset of Fig. 7), the critical field is estimated to be about 7.2 kOe. To further inspect the magnetic behavior, the field cooled magnetization curves of **1**-(*RR*) were measured under several fields as plotted inset of Fig. 6. A maximum of χ_M was observed at about 3.4 K under 5 kOe, indicating antiferromagnetism of **1**-(*RR*) under this condition. The maximum broadens and shifts to lower temperature as the magnetic field increases, and it finally disappears for $H \geq$ 11 kOe. This behavior shows the existence of a field-induced magnetic phase transition.

To investigate the phase transition at low temperature, ZFC and FC curves show abrupt increases below 3.0 K and have a divergence (Fig. 8), suggesting the occurrence of the long-range magnetic ordering below this temperature. Furthermore,

alternating current (ac) magnetic susceptibilities measurements were carried out at zero direct current (dc) field (Fig. 9). The results show that both in-phase (χ_M') and in the out-of-phase (χ_M'') signals display a peak around 3.0 K, demonstrating the field-induced three-dimensional ferromagnetic magnetic ordering below this temperature.[11c] The magnetic ordering behavior is further confirmed by the observation of hysteresis loops. As depicted in Fig. 10, the coercive field of these loops for **1**-(*RR*) increase upon cooling, and exhibit strong sweep-rate dependence, suggesting the presence of QTM (quantum tunneling of magnetization) that the tunneling can be diminished as the field sweeping rate is increased.

The magnetic susceptibility data for **2**-(*RR*) were collected at 1 kOe, as plotted in Fig. 11. At 300 K, the $\chi_M T$ value of 3.26 $cm^3 \cdot K \cdot mol^{-1}$ for per $Ru^{III}Mn^{III}$ unit is lower than the spin-only value (3.38 $cm^3 \cdot K \cdot mol^{-1}$) expected for a magnetically diluted spin system (one S_{Ru}= 1/2, one S_{Mn}= 2) with g = 2. The abrupt decrease of $\chi_M T$ below 25 K suggest the presence of antiferromagnetic coupling between Ru(III) and Mn(III) via C≡N bridges. The magnetic susceptibility obey the *Curie-Weiss* Law above 50 K with C = 3.32 $cm^3 \cdot K \cdot mol^{-1}$ and θ = −4.86 K, further confirming the presence of antiferromagnetic coupling between Ru(III) and Mn(III) ions (inset of Fig. 11). The magnetization of this compound per [$Ru^{III}Mn^{III}$] unit reaches 2.98 Nβ mol^{-1} at 70 kOe, which is smaller than the value of 3.0 Nβ with the antiferromagnetic interaction between the Ru^{III} and Mn^{III} ions. According to the structure data, the Ru^{III}–C≡N–Mn^{III} linkage is obviously different. So the susceptibility data were fitted using the expression for **1**-(*RR*), giving g_{Mn} = 1.97, g_{Ru} = 1.98, J = −1.56 cm^{-1}, α = 0.2 and zJ' = -0.04 (R = 6.04 × 10^{-4}). The fitting results indicate the dominant intramolecular antiferromagnetic interactions in **2**-(*RR*), which are comparable to the parameters obtained for analogous complexes in the literature.[4c,4e,14]

AC magnetic measurements (Figure S8, ESI†) show no detectable frequency-dependent χ_M' and χ_M'' signals for **2**-(*RR*), indicating the completely paramagnetic behavior without any magnetic ordering.

It is worth noting that the related magnetostructurally characterized analogues based on Ru^{III}–Mn^{III} systems were found to be either ferro- or antiferromagnetic

coupling (Table 4). For the nature of Ru^{III} and Mn^{III} interaction, it is expected that when the d_π orbitals on Ru^{III} and Mn^{III} are overlapped, antiferromagnetic interactions (J_{AF}) will emerge. In contrast, the Ru d_π orbitals and Mn d_z^2 orbital are orthogonal because of π/σ-type symmetry, which is expected to provide ferromagnetic routes (J_F). The orbital overlaps (J_{AF}) would be substantially reduced as inferred from the relatively long Mn-N(cyanide) length and the bent Mn–N≡C (cyanide) angles largely deviated from 180°.[24] As shown in Table 6, the bond lengths of Mn–N(cyanide) in **1**-(*RR*) (2.325(4), 2.354(4) Å), **2**-(*RR*) (2.331(6), 2.349(7) Å) are slightly larger than those in $[Ru^{III}(salen)(CN)_2][Mn^{III}(L)]$[4c] (L = N,N'-(1-methylethylene)bis(2-hydroxynaphthalene-1-carbaldehydeneiminate)dianion) (2.292(8) and 2.307(8) Å); however, the bond angles of Mn–N≡C(cyanide) (156.4(4)°, 154.3(4)°for **1**-(*RR*), 158.7(6),174.8(6)° for **2**-(*RR*)) are remarkably larger than those of $[Ru^{III}(salen)(CN)_2][Mn^{III}(L)]$[4c] (144.3(8)° and 143.1(8)°). The magnetic behavior of **1**-(*RR*) and **2**-(*RR*) are consistent with the theoretical prediction for antiferromagnetic coupling. Moreover, compared to **1**-(*RR*), the bond angles of Mn–N≡C angles of **2**-(*RR*) are closer to 180°, resulting the J_{exp} value of **2**-(*RR*) is larger than that in **1**-(*RR*).

Conclusions

In summary, with the use of dicyanoruthenate, $[Ru(salen)(CN)_2]^-$**,** as building block, two pair of enantiomorphous chiral complexes were synthesized. Vibrational circular dichroism (VCD) and Circular dichroism (CD) spectra confirm the enantiomeric properties and optically activity of **1**-(*RR*) and **1**-(*SS*), **2**-(*RR*) and **2**-(*SS*). Magnetic studies show that antiferromagnetic couplings are operative between Ru^{III} and Mn^{III} centers bridged by cyanide. Notably, compound **1**-(*RR*) shows interesting metamagnetic behavior with a critical field of about 7.2 kOe at 1.9 K. Magnetostructural correlation for some typical cyano-bridged heterobimetallic Ru^{III}–Mn^{III} compounds is discussed. Further work on chiral cyano-bridged bimetallic systems aiming at molecular multiferroic materials and chiral magnets is underway in our laboratory.

Acknowledgments

This work was supported by the Major State Basic Research Development Program (2013CB922100 and 2011CB808704), the National Natural Science Foundation of China (91022031), and the Natural Science Foundation of Jiangsu Province (BK20130054). We also thank Prof. You Song and Dr Tian-Wei Wang for experimental assistance with magnetic measurements.

Supporting Information

Additional structures, spectroscopic data and magnetic characterization data, and X-ray crystallographic files in CIF format for all complexes. This material is available free of charge via the Internet at http://www.rsc.org.

References

1 (a) R. Sessoli, H. L. Tsai, A. R. Schake, S. Wang, J. B. Vincent, K. Folting, D. Gatteschi, G. Christou, D. N. Hendrickson, *J. Am. Chem. Soc.*, 1993, **115**, 1804; (b) S. Hill, R. S. Edwards, N. Aliaga-Alcalde, G. Christou, *Science*, 2003, **302**, 1015; (c) N. Roch, S. Florens, V. Bouchiat, W. Wernsdorfer, F. Balestro, *Nature*, 2008, **453**, 633; (d) G. A. Timco, S. Carretta, F. Troiani, F. Tuna, R. G. Pritchard, E. J. L. McInnes, A. Ghirri, A. Candini, P. Santini, G. Amoretti, M. Affronte, R. E. P. Winpenny, *Nat. Nanotechnol.*, 2009, **4**, 173; (e) H. -L. Sun, Z. -M. Wang, S. Gao, *Coord. Chem. Rev.*, 2010, **254**, 1081; (f) F. Troiani, M. Affronte, *Chem. Soc. Rev.*, 2011, **40**, 3119; (g) J. M. Clemente-Juan, E. Coronado, A. Gaita-Ariño, *Chem. Soc. Rev.*, 2012, **41**, 7464.

2 (a) C. -F. Wang, J. -L. Zuo, B. M. Bartlett, S. You, J. R. Long, X. -Z. You, *J. Am. Chem. Soc.*, 2006, **128**, 7162; (b) S. Wang, J. -L. Zuo, H. -C. Zhou, H. J. Choi, Y. X. Ke, J. Long, X. -Z. You, *Angew. Chem. Int. Ed.*, 2004, **43**, 5940-5943; (c) H. -B. Zhou, J. Wang, H. -S. Wang, Y. -L. Xu, X. -J. Song, Y. Song, X. -Z. You, *Inorg. Chem.*, 2011, **50**, 6868; (d) H.-Z. Kou, B. C. Zhou, D.-Z. Liao, R.-J. Wang, Y. Li, *Inorg. Chem.*, 2002, **41**, 6887; (e) H. S. Yoo, H. H. Ko, D. W. Ryu, J. W. Lee, J. H. Yoon, W. R. Lee, H. C. Kim, E. K. Koh, C. S. Hong, *Inorg. Chem.*, 2009, **48**, 5617.

3 (a) J. J. Sokol, A. G. Hee, J. R. Long, *J. Am. Chem. Soc.*, 2002, **124**, 7656; (b) W. F. Yeung, W. L. Man, W. T. Wong, T. C. Lau, S. Gao, *Angew. Chem., Int, Ed.*, 2001, **40**, 3031; (c) X.-W. Feng, C. Mathonière, I. -R. Jeon, M. Rouzières, A. Ozarowski, M. L. Aubrey, M. I. Gonzalez, R. Clérac, J. R. Long, *J. Am. Chem. Soc.*, 2013, **135**, 15880.

4 (a) J. H. Yoon, J. W. Lee, D. W. Ryu, S. Y. Choi, S. W. Yoon, B. J. Suh, E. K. Koh, H. C. Kim, C. S. Hong, *Inorg. Chem.*, 2011, **50**, 1130; (b) M. P. Shores, J. J. Sokol, J. R. Long, *J. Am. Chem. Soc.*, 2002, **124**, 2279; (c) J. H. Yoon, H. S. Yoo, H. C. Kim, W. S. Yoon, B. J. Suh, C. S. Hong, *Inorg. Chem.*, 2009, **48**, 816; (d) S. W. Choi, Kwak, H. Y.; Yoon, J. H.; Kim, H. C.; Koh, E. K.; Hong, C. S. *Inorg. Chem.* 2008, **47**, 10214; (e) J. Xiang, L. -H. Jia, B. -W. Wang, S. -M. Yiu, S. -M. Peng, W. -Y. Wong, S. Gao, T. C. Lau, *Dalton Trans.* 2013, **42**, 3876; (f) J. Xiang, L. -H. Jia, W. -L. Man, K. Qian, S. M. Yiu, G. H. Lee, S. -M. Peng, S. Gao, T. C. Lau, *Chem. Commun.*, 2011, **47**, 8694.

5 (a) E. J. Schelter, J. K. Bera, J. Bacsa, J. R. Galán-Mascarós, and K. R. Dunbar, *Inorg. Chem.*, 2003, **42**, 4256; (b) E. J. Schelter, A. V. Prosvirin, W. M. Reiff, and K. R. Dunbar, *Angew. Chem., Int. Ed.*, 2004, **43**, 4912; (c) E. J. Schelter, A. V. Prosvirin, and K. R. Dunbar, *J. Am. Chem. Soc.*, 2004, **126**, 15004; (d) E. J. Schelter, F. Karadas, C. Avendano, A. V. Prosvirin, W. Wernsdorfer, and K. R. Dunbar, *J. Am. Chem. Soc.*, 2007, **129**, 8139; (e) K. R. Dunbar, E. J. Schelter, A. V. Palii, S. M. Ostrovsky, V. Y. Mirovitskii, J. M. Hudson, M. A. Omary, S. I. Klokishner, and B. S. Tsukerblat, *J. Phys. Chem. A.*, 2003, **107**, 11102.

6 (a) X. -Y. Wang, C. Avendaño, K. R. Dunbar, *Chem. Soc. Rev.*, 2011, **40**, 3213; (b) T. D. Harris, M. V. Bennett, R. Clérac, J. R. Long, *J. Am. Chem. Soc.*, 2010, **132**, 3980; (c) M. P. Shores, J. J. Sokol, and J. R. Long, *J. Am. Chem. Soc.*, 2002, **124**, 2279; (d) D. E. Freedman, D. M. Jenkins, and J. R. Long, *Chem. Commun.*, 2009, 4829.

7 (a) E. V. Peresypkina, A. Majcher, M. Rams, K. E. Vostrikova, *Chem. Commun.*, 2014, **50**, 7150; (b) V. S. Mironov, L. F. Chibotaru, A. Ceulemans, *J. Am. Chem. Soc.*, 2003, **125**, 9750; (c) V. S. Mironov, *Dokl. Phys. Chem.*, 2006, **408**, 130;(d)

V. Mironov, *Dokl. Phys. Chem.*, 2007, **415**, 199.

8 (a) G. Rogez, C. Massobrio, P. Rabu, M. Drillon, *Chem. Soc. Rev.*, 2011, **40**, 1031. (b) M. Clemente-León, E. Coronado, C. Martí-Gastaldo, F. M. Romeroab, *Chem. Soc. Rev.*, 2011, **40**, 473; (c) R. Sessoli, M. G. Pini, A. Rettori, M. A. Novak, P. Rosa, M. Massi, M. E. Fedi, L. Giuntini, A. Caneschi, D. Gatteschi, *Phys. Rev. B: Condens. Matter Mater. Phys.*, 2005, **72**, 64406; (d) C. Train, M. Gruselle, M. Verdaguer, *Chem. Soc. Rev.*, 2011, **40**, 3297; (e) L. D. Barron, *Nat. Mater.*, 2008, **7**, 691.

9 (a) W. Kaneko, S. Kitagawa, M. Ohba, *J. Am. Chem. Soc.*, 2007, **129**, 248; (b) M. Clemente-León, E. Coronado, J. C. Dias, A. Soriano-Portillo, R. D. Willett, *Inorg. Chem.*, 2008, **47**, 6458; (c) D. -R. Xiao, G. -J. Zhang, J. -L. Liu, L. -L. Fan, R. Yuan, M. -L. Tong, *Dalton Trans.*, 2011, **40**, 5680; (d) L. -L. Fan, F. -S. Guo, L. Yuan, Z. -J. Lin, R. Herchel, J. D. Leng, Y. G. Ou, M. L. Tong, *Dalton. Trans.*, 2010, 1771; (e) Y. -Y. Zhu, X. Guo, C. Cui, B. -W. Wang, Z. -M. Wang, S. Gao, *Chem. Commun.*, 2011, **47**, 8049.

10 (a) P. Gerbier, N. Domingo, J. Gomez-Segura, D. Ruiz-Molina, D. B. Amabilino, J. Tejada, B. E. Williamson, J. Veciana, *J. Mater. Chem.*, 2004, **14**, 2455; (b) C. M. Zaleski, E. C. Depperman, J. W. Kampf, M. L. Kirk, V. L. Pecoraro, *Inorg. Chem.*, 2006, **45**, 10022.

11 (a) H. -R. Wen, C. -F. Wang, Y. -Z. Li, J. -L. Zuo, Y. Song, X. –Z. You, *Inorg. Chem.*, 2006, **45**, 7032; (b) M.-X. Yao, Q. Zheng, X.-M. Cai, Y.-Z. Li, Y. Song, J.-L. Zuo, *Inorg. Chem.*, 2012, **51**, 2140; (c) D. -P. Zhang, Y. -Z. Bian, J. Qin, P. Wang, X. Chen, *Dalton Trans.*, 2014**, 43**, 945; (d) M.-X. Yao, Q. Zheng, F. Gao, Y. -Z. Li, J. -L. Zuo, *Sci. China Chem.*, 2012, **55**, 1022; (e) H. Imai, K. Inoue, K. Kikuchi, Y. Yoshida, M. Ito, T. Sunahara, S. Onaka, *Angew. Chem., Int. Ed.*, 2004, **43**, 5618; (f) K. Inoue, K. Kikuchi, M. Ohba, H. Õkawa, *Angew. Chem., Int. Ed.*, 2003, **42**, 4810; (g) M. Minguet, D. Luneau, E. Lhotel, V. Villar, C. Paulsen, D. B. Amabilino, J. Veciana, *Angew. Chem., Int. Ed.*, 2002, **41**, 586.

12 (a) J. Milon, M. C. Daniel, A. Kaiba, P. Guionneau, S. Brandès, J. P. Sutter, *J. Am. Chem. Soc.*, 2007, **129**, 13872; (b) O. Stefańczyk, M. Rams, A. M. Majcher, C. Mathonière, B. Sieklucka, *Inorg. Chem.*, 2014, **53**, 3874.

13 (a) E. Coronado, C. J. Gómez-García, A. Nuez, F. M. Romero, E. Rusanov, H. Stoeckli-Evans, *Inorg. Chem.*, 2002, **41**, 4615; (b) K. Inoue, H. Imai, P. S. Ghalsasi, K. Kikuchi, M. Ohba, H. Okawa, J. V. Yakhmi, *Angew. Chem., Int. Ed.*, 2001, **40**, 4242; (c) K. Inoue, K. Kikuchi, M. Ohba, H. Okawa, *Angew. Chem., Int. Ed.*, 2003, **42**, 4709.

14 J. Ru, F. Gao, T. Wu, M. -X. Yao, Y.-Z. Li, J.-L. Zuo, *Dalton Trans.*, 2014, **43**, 933.

15 P. Pfeifer, T. Hesse, H. Pfitzner, W. Scholl, H. Thielert, *J. Pract. Chem.*, 1937, **149**, 217.

16 W. H. Leung, C. M. Che, *Inorg. Chem.*, 1989**, 28,** 4619**.**

17 *SAINT-Plus*, version 6.02; Bruker Analytical X-ray System: Madison, WI, 1999.

18 Sheldrick, G. M. *SADABS an empirical absorption correction program*; Bruker Analytical X-ray Systems: Madison, WI, 1996.

19 G. M. Sheldrick, *SHELXTL-97*; Universität of Göttingen: Göttingen, Germany, 1997.

20 (a) T. Wu, X. -P. Zhang, C. -H. Li, P. Bouř, Y. -Z. Li, X. -Z. You, *Chirality*, 2012, **24**, 451; (b) T. Wu, X. -Z. You, *J. Phys. Chem. A.*, 2012, **116**, 8959.

21 (a) O. Rotthaus, O. Jarjayes, F. Thomas, C. Philouze, E. Saint-Aman and J.-L. Pierre, *Dalton Trans.*, 2007, 889; (b) J. C. Wu, S.-X. Liu, T. D. Keene, A. Neels, V. Mereacre, A. K. Powell, and S. Decurtins, *Inorg. Chem.*, 2008, **47**, 3452.

22 (a) L. A. Nafie, Vibrational Optical Activity: Principles and Applications, J. Wiley & Sons, Chichester, 2011; (b) G. Tian, G. -S. Zhu, X. -Y. Yang, Q. -R. Fang, M. Xue, J. -Y. Sun, Y. Wei, and S. -L. Qiu, *Chem. Commun*., 2005, 1396; (c) C. Johannessen, P. W. Thulstrup, *Dalton Trans.*, 2007, 1028; (d) T. Wu, C. -H. Li, Y. Z. Li, Z. -G. Zhang, X. -Z.You, *Dalton Trans.*, 2010, **39**, 3227.

23 O. Kahn, Molecular Magnetism; VCH: Weinhem, Germany, 1993.

24 H. Miyasaka, A. Saitoh, S. Abe, *Coord. Chem. Rev*., 2007, **251**, 2622.

Table 1 Summary of crystallographic data for all complexes

	1-(*RR*)	**1-(*SS*)**	**2-(*RR*)**	**2-(*SS*)**
formula	$C_{38}H_{34}MnN_6O_4Ru$	$C_{38}H_{34}MnN_6O_4Ru$	$C_{92}H_{72}Mn_2N_{12}O_8Ru_2$	$C_{92}H_{72}Mn_2N_{12}O_8Ru_2$
fw	794.72	794.72	1785.64	1785.64
crystal system	Monoclinic	Monoclinic	Triclinic	Triclinic
space group	$P2_1$	$P2_1$	$P1$	$P1$
a, Å	10.8040(13)	10.8146(15)	13.2812(13)	13.3357(16)
b, Å	13.3524(16)	13.3776(18)	20.8357(15)	20.7715(14)
c, Å	12.7899(15)	12.8080(17)	20.9023(15)	21.0323(14)
α, deg	90	90	100.140(2)	100.669(2)
β, deg	97.497(2)	97.643(2)	104.427(3)	104.517(3)
γ, deg	90	90	107.371(2)	106.257(2)
V, Å^3	1829.3(4)	1836.5(4)	5146.3(7)	5206.2(8)
Z	2	2	2	2
ρ_{calcd}, g cm^{-3}	1.433	1.437	1.152	1.139
T / K	296(2)	293(2)	291(2)	291(2)
μ, mm^{-1}	0.805	0.802	0.580	0.573
θ, deg	1.61 to 25.50	1.60 to 25.01	1.04 to 26.00	1.32 to 25.00
F(000)	810	810	1820	1820
index ranges	$-13 \le h \le 13$ $-14 \le k \le 16$ $-15 \le l \le 15$	$-12 \le h \le 12$ $-15 \le k \le 9$ $-15 \le l \le 15$	$-16 \le h \le 16$ $-25 \le k \le 25$ $-16 \le l \le 25$	$-16 \le h \le 17$ $-26 \le k \le 26$ $-26 \le l \le 16$
data/restraints /parameters	6025 / 1 / 451	4768 / 1 / 404	27368 / 3 / 2089	30548 / 3 / 2089
GOF (F^2)	1.061	1.065	1.061	1.096
$R_1{}^a$,$wR_2{}^b$ (I>2σ(I))	0.0369, 0.0984	0.0772, 0.1856	0.0552, 0.1482	0.0578, 0.1393
$R_1{}^a$, $wR_2{}^b$ (all data)	0.0431, 0.1029	0.0817, 0.1897	0.0593, 0.1492	0.0656, 0.1408

$R_1{}^a = \Sigma||F_o| - |F_c||/\Sigma F_o|$. $wR_2{}^b = [\Sigma w(F_o{}^2 - F_c{}^2)^2/\Sigma w(F_o{}^2)^2]^{1/2}$

Table 2 Selected bond lengths (Å) and angles (°) for complex **1-(*RR*)**

Ru(1)-N(2)	1.994(4)	Ru(1)-N(1)	2.008(5)
Ru(1)-C(38)	2.066(4)	Ru(1)-C(37)	2.091(4)
Mn(1)-N(4)	1.963(5)	Mn(1)-N(3)	2.002(4)
Mn(1)-N(5)	2.325(4)	Mn(1)-N(6)	2.354(4)
N(2)-Ru(1)-N(1)	82.57(17)	N(2)-Ru(1)-O(2)	170.53(17)
N(1)-Ru(1)-O(2)	89.87(16)	N(2)-Ru(1)-O(1)	90.93(17)
N(1)-Ru(1)-O(1)	172.93(17)	O(2)-Ru(1)-O(1)	96.86(14)
C(1)-N(1)-Ru(1)	127.3(4)	C(8)-N(1)-Ru(1)	112.9(3)
C(16)-N(2)-Ru(1)	126.0(4)	C(9)-N(2)-Ru(1)	113.9(3)
N(6)#1-C(37)-Ru(1)	175.4(6)	N(5)-C(38)-Ru(1)	174.2(4)
C(36)-N(4)-Mn(1)	125.0(4)	C(29)-N(4)-Mn(1)	112.6(3)
C(38)-N(5)-Mn(1)	156.4(4)	C(37)#2-N(6)-Mn(1)	154.3(4)
C(23)-N(3)-Mn(1)	124.8(4)	C(24)-N(3)-Mn(1)	112.1(3)

Symmetry transformations used to generate equivalent atoms: #1 x−1, y, z; #2 x+1, y, z

Table 3 Selected bond lengths (Å) and angles (°) for complex **2-(*RR*)**

C(89)-Ru(2)#1	2.080(7)	C(90)-Ru(1)	2.017(7)
C(91)-Ru(1)	2.136(6)	C(92)-Ru(2)	2.008(7)
Mn(1)-O(1)	1.986(5)	Mn(1)-N(2)	2.019(5)
Mn(1)-N(1)	2.065(6)	Mn(1)-O(2)	2.070(5)
Mn(1)-N(9)	2.272(6)	Mn(1)-N(10)	2.299(6)
Mn(4)-N(21)	2.236(6)	Mn(4)-N(22)	2.297(6)
Mn(4)-N(13)	2.044(5)	Mn(4)-N(14)	1.977(6)
Mn(3)-N(23)	2.331(6)	Mn(3)-N(24)	2.349(7)
Mn(3)-N(18)	2.010(6)	Mn(3)-N(17)	2.016(5)
N(3)-Ru(1)	2.076(6)	N(4)-Ru(1)	2.011(5)
O(3)-Ru(1)	2.037(4)	O(4)-Ru(1)	2.068(4)
N(10)-C(90)-Ru(1)	174.6(5)	N(11)-C(91)-Ru(1)	171.9(5)
N(24)-C(184)-Ru(4)	167.4(6)	N(12)-C(92)-Ru(2)	178.0(5)
N(22)-C(182)-Ru(3)	176.9(6)	N(23)-C(183)-Ru(3)	173.3(6)
C(7)-N(1)-Mn(1)	124.2(3)	C(8)-N(1)-Mn(1)	103.1(3)
C(10)-N(2)-Mn(1)	119.4(3)	C(9)-N(2)-Mn(1)	106.3(3)
C(89)-N(9)-Mn(1)	171.0(5)	C(90)-N(10)-Mn(1)	166.0(4)
C(1)-O(1)-Mn(1)	128.4(3)	C(16)-O(2)-Mn(1)	129.0(3)
C(183)-N(23)-Mn(3)	158.7(6)	C(184)-N(24)-Mn(3)	174.8(6)
C(29)-O(3)-Ru(1)	119.3(3)	C(44)-O(4)-Ru(1)	126.4(3)

Symmetry transformations used to generate equivalent atoms: #1 x, y, z+1.

Table 4 Structural and Magnetic Parameters for some cyano-bridged Ru^{III}-Mn^{III} Complexes[a]

Complexes	d_{Mn-N}/ Å	Ru-C-N(deg)	Mn-N-C(deg)	J_{exp}/cm^{-1}	ref
Ru(salen)CN_2[Mn(L)]	2.292-2.307	169.9-170.6	143.1-144.3	1.34	4c
{[Ru(Q)$_2$](μ-CN)$_2$[Mn(salcy)]}$_n$	2.286-2.302	174.3-176.6	149.6-154.2	−0.75	4e
(*R*,*R*)[Ru(5-Cl-Salcy)($CN)_2$Mn(salen)]$_n$	2.306-2.355	170.3-178.0	147.3-167.8	−8.37, −8.80	14
[Ru(salen)$(CN)_2$Mn(*R*,*R*-salcy)]$_n$	2.325-2.354	174.2-175.4	156.4- 154.3	−0.40, −1.32	This paper
[Ru(salen)$(CN)_2$Mn(*R*,*R*-salphen)]$_n$	2.331-2.349	168.9-178.0	158.7-174.8 166.0-171.0	−1.25, −1.87	This paper

[a]Abbreviations used for the ligands: salen = N,N'-ethylenebis(salicylideneiminato) dianion; L=N,N'-(1-methylethylene)bis(2-hydroxynaphthalene-1-carbaldehydene -iminate)dianion; Q = 8-hydroxyquinoline; salcy= N,N'-(1,2-cyclohexanediylethylene)bis (salicylideneiminato)dianion; salphen = N,N'-(1,2-diphenylethylene) bis(salicylideneiminato) dianion.

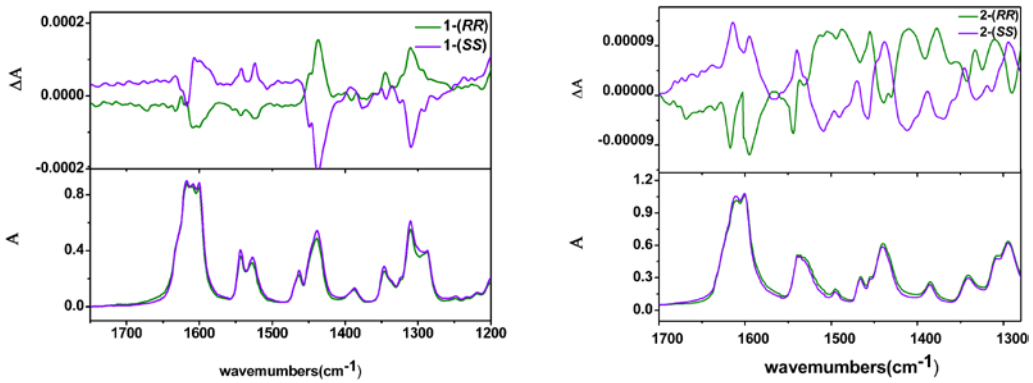

Fig. 1 Left: VCD (top) and IR absorption (bottom) spectra of **1**-(*RR*) and **1**-(*SS*). Right: VCD (top) and IR absorption (bottom) spectra of **2**-(*RR*) and **2**-(*SS*).

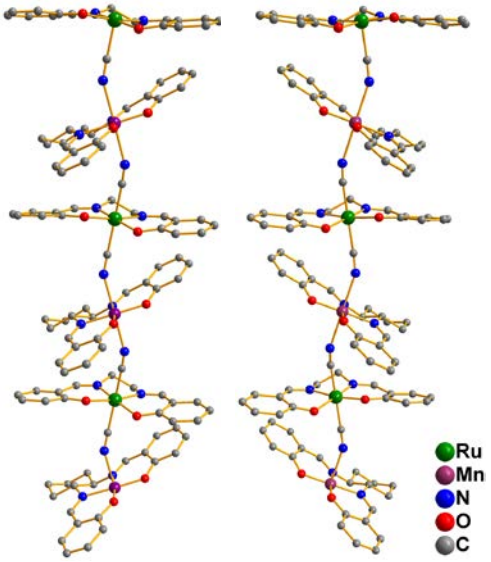

Fig. 2 Perspective view of one-dimensional zigzag infinite chains of **1**-(*RR*) and **1**-(*SS*), respectively. Hydrogen atoms are omitted for clarity.

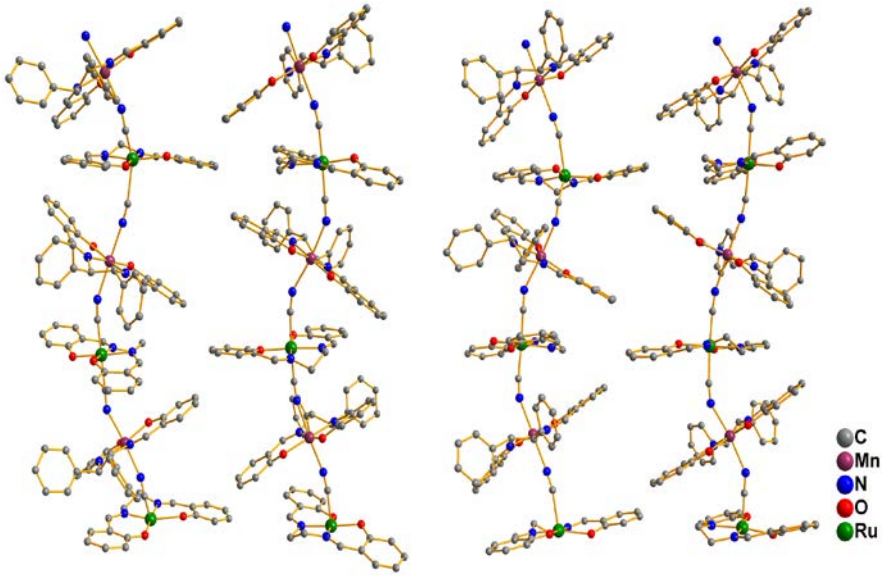

Fig. 3 Perspective view of one-dimensional zigzag infinite chains of **2**-(*RR*) and **2**-(*SS*), respectively. Hydrogen atoms are omitted for clarity.

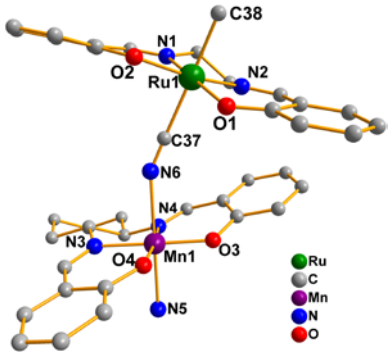

Fig. 4 Perspective drawing of the crystallographically structural of unit of **1**-(*RR*)

showing the atom numbering. Hydrogen atoms are omitted for clarity.

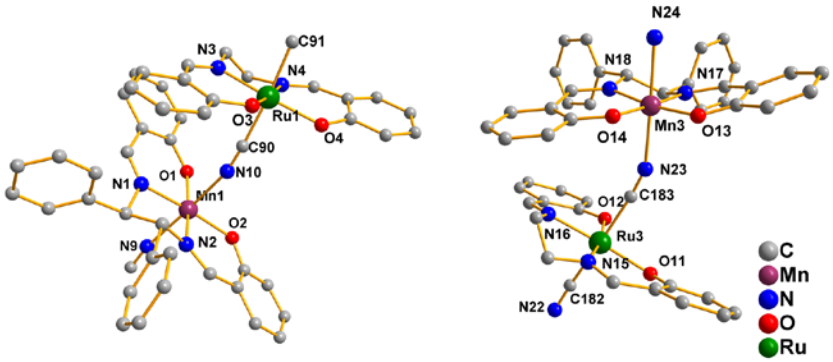

Fig. 5 Perspective drawing of the crystallographically structural of unit of **2**-(RR) showing the atom numbering. Hydrogen atoms are omitted for clarity.

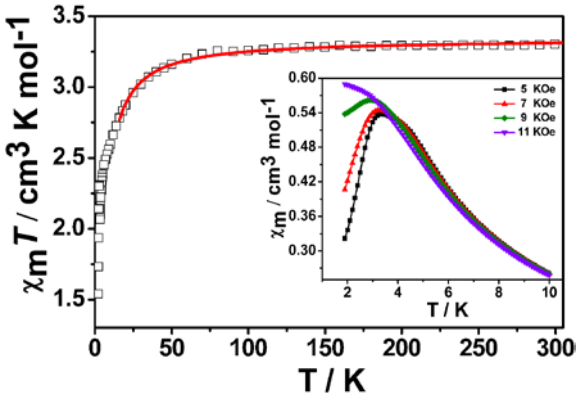

Fig. 6 Temperature dependence of the $\chi_M T$ product for **1-(*RR*)** at 1KOe. The red solid line represents the best fits of the data. (Inset) Thermal dependence of the magnetic susceptibility at T≤10 K.

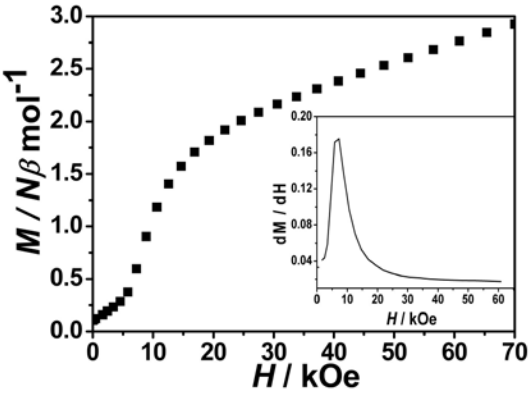

Fig. 7 Field dependence of magnetization at 1.9 K for **1**-(*RR*). (Inset) d*M*/d*H vs H* plot.

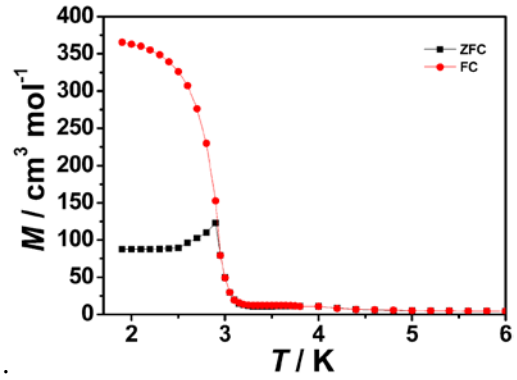

Fig. 8 Temperature dependence of the magnetization for **1** at 10 Oe. ZFC (■) and FC (●)

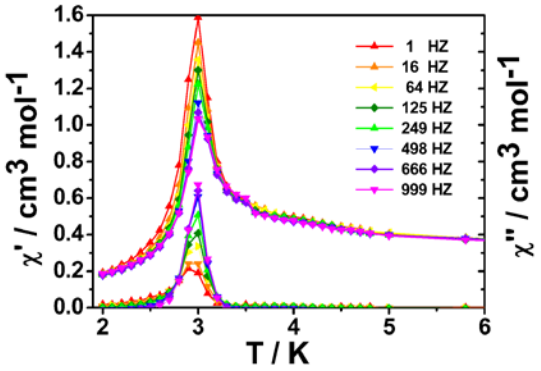

Fig. 9 Temperature dependence of the in-phase χ' (top) and out-of-phase χ'' (bottom) at different frequencies in 2 Oe ac field oscillating at 1-999 Hz with zero applied dc field for **1**-(*RR*).

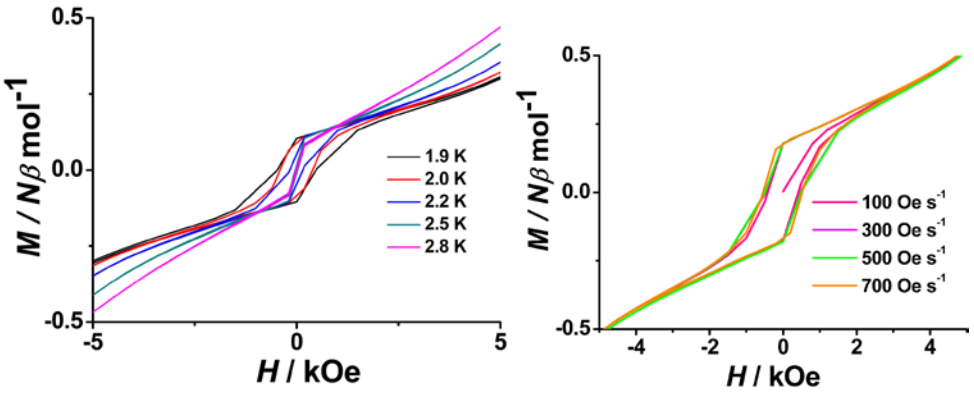

Fig. 10 Temperature- and field- sweep rate-dependent magnetic hysteresis loops for powder of **1**-(*RR*) measured at the indicated conditions.

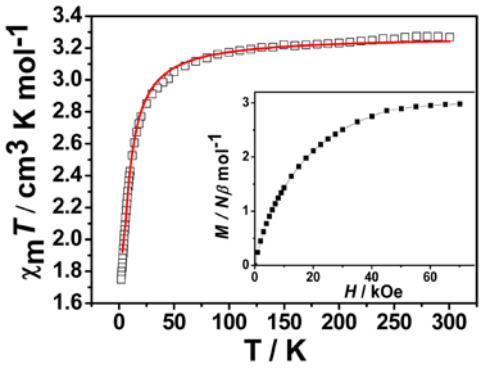

Fig. 11 Temperature dependence of the $\chi_M T$ product for **2**-(*RR*) at 1 kOe. The red solid line represents the best fits of the data. (Inset) Field dependence of the magnetization of **2**-(*RR*) at 1.9 K.

Graphic Abstract

Two pairs of one-dimesinal enantiomers based on the chiral Mn^{III} Schiff-base complexes and the dicyanoruthenate building block, $[Ru(salen)(CN)_2]^-$, have been synthesized and structurally characterized. Vibrational circular dichroism (VCD) and circular dichroism (CD) spectra confirm their enantiomeric properties. Magnetic studies show that antiferromagnetic couplings are operative between Ru^{III} and Mn^{III} centers bridged by cyanide. **1**-(*RR*) shows the interesting metamagnetic behavior with a critical field of about 7.2 kOe at 1.9 K. Magnetostructural correlation for some typical cyano-bridged heterobimetallic Ru^{III}–Mn^{III} compounds is discussed.